

Spectroscopic study of odd-parity excited levels of atomic gadolinium in the 28700-31500 cm^{-1} region using a three-color three-step resonance ionization pathway

Jun-Yao Zhang(张钧尧), Kai-Chen Ma(马恺宸), Jing-Yi Xiong(熊静逸), Li-De Wang(王立德), Cai-Hua Zhu(朱才华), Jun-Jie Chai(柴俊杰), and Yun-Fei Li(李云飞)

Citation: Chin. Phys. B, 2026, 35 (**7**): 073201. DOI: 10.1088/1674-1056/ae12dd
http://cpb.iphy.ac.cn; http://iopscience.iop.org/cpb

What follows is a list of articles you may be interested in

Angular momentum distribution of atomic hydrogen in excited states under ultra-short laser field

Zhaoyan Zhou(周兆妍), Dongwen Zhang(张栋文), and Zengxiu Zhao(赵增秀)
Chin. Phys. B, 2026, 35 (**3**): 033201. DOI: 10.1088/1674-1056/adfdc6

New spectroscopic data on even-parity autoionization states for two-color two-step photoionization of nickel atom

Jun-Yao Zhang(张钧尧), Jing-Yi Xiong(熊静逸), Hong-Ru Zhou(周鸿儒), Cai-Hua Zhu(朱才华), Huai-Miao Sun(孙槐苗), Li-De Wang(王立德), Kai-Chen Ma(马恺宸), Jun-Jie Chai(柴俊杰), and Yun-Fei Li(李云飞)
Chin. Phys. B, 2026, 35 (**1**): 013201. DOI: 10.1088/1674-1056/adf4ae

Influence of excited states in high-order harmonic generation at intense mid-infrared field

Yan Fang(方言), Da-Wei Tian(田大纬), Yue Cao(曹玥), Xiao-Lei Hao(郝小雷), and Zheng Shu(舒正)
Chin. Phys. B, 2025, 34 (**10**): 103201. DOI: 10.1088/1674-1056/adda0d

Role of excited states in helium-like ions on high-order harmonic generation

Jiang-Hua Luo(罗江华) and Jia-Jun Xiao(肖佳俊)
Chin. Phys. B, 2023, 32 (**11**): 113201. DOI: 10.1088/1674-1056/ace317

Quantum control of ultrafast magnetic field in H_3^{2+} molecules by tricircular polarized laser pulses

Qing-Yun Xu(徐清芸), Yong-Lin He(何永林), Zhi-Jie Yang(杨志杰), Zhi-Xian Lei(雷志仙),Shu-Juan Yan(闫淑娟), Xue-Shen Liu(刘学深), and Jing Guo(郭静)
Chin. Phys. B, 2023, 32 (**3**): 033202. DOI: 10.1088/1674-1056/ac90b6

DATA PAPER

Spectroscopic study of odd-parity excited levels of atomic gadolinium in the 28700–31500 cm^{-1} region using a three-color three-step resonance ionization pathway

Jun-Yao Zhang(张钧尧)[1,2,3], Kai-Chen Ma(马恺宸)[2], Jing-Yi Xiong(熊静逸)[2], Li-De Wang(王立德)[1,2,3], Cai-Hua Zhu(朱才华)[2], Jun-Jie Chai(柴俊杰)[1,2,3], and Yun-Fei Li(李云飞)[1,2,†]

[1] *National Key Laboratory of Particle Transport and Separation Technology, Tianjin* 300180, *China*
[2] *Research Institute of Physical and Chemical Engineering of Nuclear Industry, Tianjin* 300180, *China*
[3] *Tianjin Key Laboratory of Stable Isotope Materials Technology, Tianjin* 300180, *China*

(Received 6 September 2025; revised manuscript received 10 October 2025; accepted manuscript online 14 October 2025)

The three-color, three-step resonance ionization spectroscopy technique was employed to investigate the odd-parity excited states of gadolinium in the 28700–31500 cm^{-1} energy region. Spectra scanned without λ_1 led to the identification of 101 interference peaks, which were excluded from subsequent studies. A total of 40 odd-parity excited states were observed from scans of nine even-parity lower levels, including 19 states reported here for the first time. Unique J values were assigned to 39 levels using the electric dipole selection rule. Comparison with previous studies confirms the reliability of the present results, with the absolute energy accuracy estimated to be better than ±0.1 cm^{-1}.

Keywords: atomic gadolinium, excited states, odd-parity, resonance ionization

PACS: 32.80.Zb, 82.80.Ms, 42.55.Mv

DOI: 10.1088/1674-1056/ae12dd **CSTR:** 32038.14.CPB.ae12dd

1. Introduction

High-lying excited states of rare-earth elements have long attracted interest owing to their importance in atomic structure studies,[1–3] laser isotope separation,[4–6] and astrophysical modeling.[7–9] Despite extensive spectroscopic efforts, the energy-level structures of many lanthanide atoms remain only partially explored, particularly above 30000 cm^{-1} . Gadolinium (Gd), with its half-filled 4f^7 shell and multiple optically active valence electrons, exhibits one of the most intricate spectra among lanthanides. Beyond its spectroscopic intricacy, accurate atomic data on Gd I are essential for astrophysical applications. In particular, Gd abundances are regarded as tracers of r-process enrichment in the Galaxy and are vital for modeling the opacities of kilonova ejecta, where lanthanides dominate the spectral features.[10–13] Reliable excited-state energy levels are therefore critical for determining Gd abundances and refining nucleosynthesis models. Furthermore, laser isotope separation of Gd has considerable practical relevance.[14–16] As the sole source of isotopic selectivity in this process, multiphoton excitation ionization strongly depends on detailed atomic fine- and hyperfine-structure data.

Although significant progress has been made in characterizing low-lying even-parity states, research on odd-parity excited states remains limited. Early emission-spectroscopy studies identified 236 odd-parity levels and 371 even-parity levels of Gd, forming the majority of the currently cataloged states.[17] However, because higher excitation levels have very low atomic populations, the associated weak transition spectra are difficult to detect and analyze, resulting in a significant discrepancy between the number of energy levels predicted theoretically and those discovered experimentally. For example, of the levels predicted for the 4f^{7}5d^3 and 4f^{8}6s6p configurations, which are above 20000 cm^{-1}, only 31% and 36.5% were experimentally observed, respectively. This highlights the incompleteness of the current atomic Gd energy level data and the need for experimental techniques to identify potential excited states.

Laser spectroscopy techniques, such as laser resonance ionization spectroscopy (RIS), are well-suited to studying high-lying odd-parity excited states, as they can selectively pump atoms from low-lying levels to specific high-lying states. A two-color, three-step RIS scheme was first employed by Qu *et al.*[18] to probe odd-parity excited states of Gd in the 34463–35628 cm^{-1} range, yielding 11 new levels. Miyabe[19,20] systematically investigated the odd-parity excited states of Gd in the 31000–37000 cm^{-1} range, identifying 38 new levels and assigning the angular momenta for most levels using multi-level cross-scans and polarized laser pumping methods. Kim *et al.*[21] also reported 23 new odd-parity excited levels in the 35500–37700 cm^{-1} range. While these studies have substantially expanded the database of odd-parity excited states, they also underscore the incompleteness of the

†Corresponding author. E-mail: Ipce_liyf@mails.cneic.com.cn

© 2026 Chinese Physical Society and IOP Publishing Ltd. All rights, including for text and data mining, AI training, and similar technologies, are reserved.

Gd atomic structure inferred from emission spectroscopy. Notably, the spectral region below 31000 cm^{-1} has never been investigated with modern laser spectroscopy, and it has relied entirely on earlier emission studies.

In this work, the odd-parity excited states of Gd in the 28700–31500 cm^{-1} range are systematically investigated using a laser resonance ionization mass spectrometry system, starting from nine different even-parity excited states. The same experimental system has previously been used to study the structures of atomic Lu and Ni, providing a wealth of fundamental data.[22–24] In total, 19 new excited states were identified; their energy levels were measured with high precision, and their angular momenta were assigned. Our work bridges the knowledge gap by providing more comprehensive atomic structure data for Gd, thereby informing the theoretical calculation of lanthanide atomic levels and astrophysical modeling.

2. Setup

2.1. Experimental system

The experimental system, depicted in Fig. 1, was largely similar to our previous configurations,[22–24] with only slight adjustments. The dye laser system consisted of three tunable dye lasers, each pumped by a Nd:YAG solid-state laser. The Nd:YAG lasers emitted 532 nm radiation at a 10 kHz repetition rate with a pulse width of 50 ns, which was delivered to the dye lasers via optical fibers. The first dye laser excited gadolinium atoms to the first excited states, while the second was scanned in the range of 570–708.5 nm to probe higher odd-parity states. These two lasers have a maximum power of 500 mW, a spectral linewidth of approximately 1.5 GHz, and a pulse duration of 20–30 ns. Wavelength tuning was achieved by adjusting the grating position in the Littman cavity using a stepper motor. The third dye laser was frequency-doubled using nonlinear BBO crystals outside the cavity, generating UV radiation fixed at 322.5 nm with a power up to 150 mW. A portion of the light from each dye laser was coupled out of the cavity, sampled by an optical fiber, and directed to a wavelength meter (with 60 MHz absolute accuracy, calibrated periodically using Rb reference lines). The laser beams were focused into optical fibers via plano-convex lenses and then combined using a multi-channel fiber combiner, streamlining the process compared to conventional setups using dichroic mirrors. At the combiner output, an achromatic aspherical mirror assembly shaped the beam into a 2.5 mm diameter circular spot, which was focused into the acceleration region of the time-of-flight mass spectrometer (TOF-MS). The mirror was fixed in place to minimize potential drift during long-distance free-space propagation.

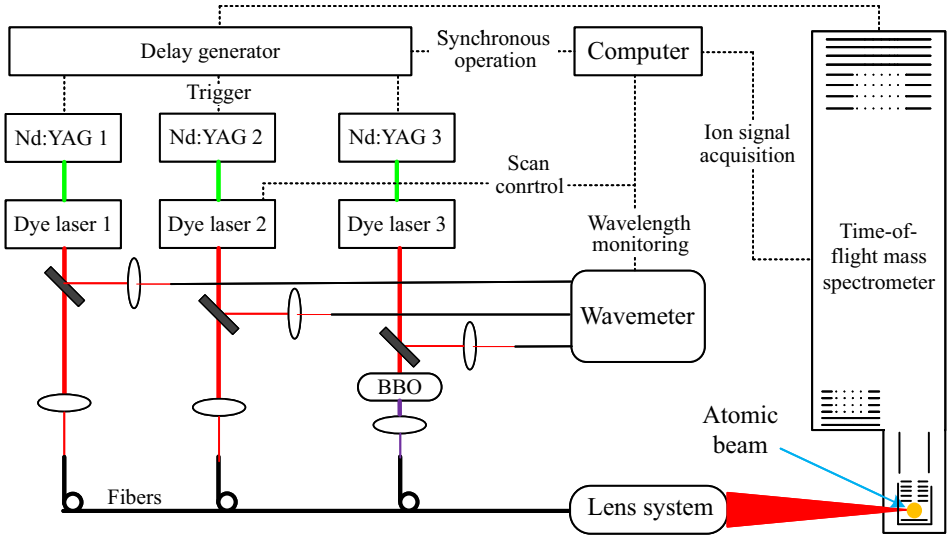


Fig. 1. Schematic of the resonance ionization mass spectrometry (RIMS) setup. A computer interfaces with the delay generator, scanning dye laser, wavemeter, and mass spectrometer via communication lines (black dashed lines). Laser beams are delivered through optical fibers (black solid lines). Integrated control software synchronizes all components, enabling wavelength scanning, real-time monitoring, and ion signal acquisition.

The TOF-MS system integrated an atomic evaporation oven with a mass analyzer within a vacuum chamber. Gadolinium metal was loaded into a tantalum capillary, where it was heated to ~ 1500 °C to generate an atomic beam. This beam passed through a slit aperture into the acceleration region, which was equipped with pulsed high-voltage electric fields. Photoionization occurred between a positively biased pulsed repelling plate and a grounded plate, triggered by a synchronized laser pulse at 10 kHz with a ~ 300 ns delay to suppress Stark effects. The positive pulse voltage was a square wave with a pulse width of 20 microseconds, and a rise time of no more than 50 ns. The directions of the laser, atomic beam, and ion repulsion were arranged orthogonally. Photoions underwent three reflections in the mass analyzer before being amplified by an electron multiplier, and the signal intensity was represented by the amplitude of the instantaneous analog voltage signal output with the unit of mV. The voltage signal was digitized by an analog-to-digital converter (ADC) and displayed as a mass spectrum on an industrial control computer, achieving a mass resolution exceeding 8000 (FWHM). Signals

primarily from ^{158}Gd were recorded, as it has the highest abundance. Laser wavelength and mass spectral data were simultaneously acquired, with signal intensity increasing at resonant wavelengths. Weak signals from non-resonant ionization by the third laser provided baseline references.

2.2. Scanning setup

The experiment employed a three-color, three-step photoionization scheme, as shown in Fig. 2. First, atoms in the ground or metastable states were pumped to a selected first excited state. The second laser was scanned over 570–708.5 nm, and when the laser wavelength matched the energy separation between the first and second excited states, atoms were pumped to the second odd-parity excited state. Subsequently, absorption of a 322.5 nm photon resulted in photoionization, producing a sharp increase in the ion signal in the mass spectrometer.

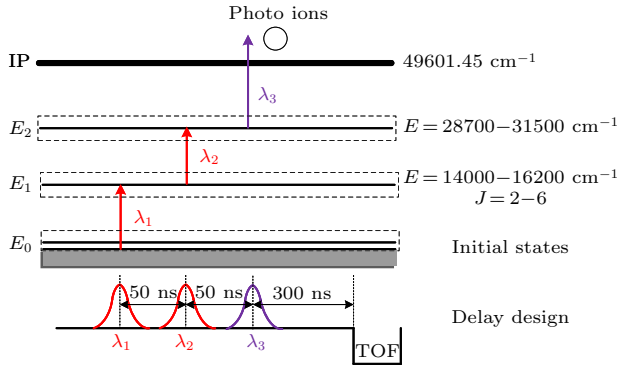


Fig. 2. Schematic of the three-color, three-step photoionization scheme. λ_1 excites atoms from the ground or metastable states to even-parity lower levels, λ_2 pumps them to target odd-parity excited states, and λ_3 (322.5 nm) ionizes; 50 ns delays are inserted between $\lambda_1 - \lambda_2$ and $\lambda_2 - \lambda_3$.

Two key aspects were considered in the experimental design:

1. The energy level structure of gadolinium is complex, with significant atomic population in low metastable states, which allows atoms to absorb multiple photons and undergo photoionization without passing through the selected first excited state.[25] This pathway interferes with the identification of the true second odd-parity excited state. Therefore:

(a) After a narrow-range scan, the λ_3 photon was fixed at 322.5 nm. At this wavelength, only very weak $2\lambda_3$ (two-photon) signals were observed. In addition, the energies of $\lambda_1 + \lambda_3$ or $\lambda_2 + \lambda_3$ from the ground state or the lowest four metastable states were insufficient to reach the ionization threshold, thereby reducing possible interference from undesired transitions.

(b) Delays of 50 ns were introduced between both $\lambda_1 - \lambda_2$ and $\lambda_2 - \lambda_3$ to avoid possible two-photon near-resonant transitions, ensuring that the transitions occurred in the intended sequence. This timing was justified because levels in the target range generally exhibit long radiative lifetimes;[26] consequently, spontaneous emission does not substantially depopulate the excited states within 50 ns.

(c) Before scanning the second excited state, a scan was performed with λ_1 blocked. Peaks observed in this scan were regarded as interference for subsequent studies of odd-parity excited states and were excluded, thereby enabling identification of the genuine second excited state.

2. To determine the total angular momentum (J) of the energy levels, it is typical to scan the same spectral range from lower levels with different J values, using the electric-dipole selection rule $\Delta J = 0, \pm 1$ to assign the J value of the upper level. However, weak transition strengths may place some transitions below the detection limit, resulting in possible misassignments of J values. To obtain unambiguous J assignments for the excited states, it is generally necessary to select as many lower levels with distinct J values as possible for scanning. For example, Miyabe employed 20 low-lying excited states to scan the odd-parity excited states of Gd in the 31000–37000 cm^{-1} range,[19] and Zhang used 8 high-lying excited states to scan the odd-parity autoionization states of Ni in the 64600–68700 cm^{-1} range.[24]

Therefore, considering the studied wavelength region, the available laser tuning range, and the NIST Atomic Spectra Database,[27] we selected nine even-parity excited states and corresponding transition schemes, as listed in Table 1, to scan the odd-parity excited states. These lower excited states fall in the 14000–16200 cm^{-1} range, with $J = 2$–6. Converging transitions from different low-lying excited states to the same odd-parity excited states provide direct evidence for new level identification, and the selection rule permits a unique J assignment for the excited states.

Table 1. Selected low-lying even-parity states and corresponding transitions used to probe odd-parity excited states.

Number	Configuration	Term	E_1 (cm^{-1})	λ_1 (nm)	P_1 (mW)
2A	$4f^7(^8S^\circ)5d\,(^9D^\circ)6s6p(^3P^\circ)$	$^{11}F_2$	14036.026	712.452	
3A	$4f^86s^2$	$^7F_3$	14253.948	701.560	
3B	$4f^7(^8S^\circ)5d\,(^9D^\circ)6s6p(^3P^\circ)$	$^{11}F_3$	14298.311	699.383	
3C	$4f^7(^8S^\circ)5d\,(^9D^\circ)6s6p(^3P^\circ)$	$^{11}D_3$	16061.273	622.616	
4A	$4f^7(^8S^\circ)5d\,(^9D^\circ)6s6p(^3P^\circ)$	$^{11}F_4$	14669.148	691.849	250
4B	$4f^7(^8S^\circ)5d\,(^9D^\circ)6s6p(^3P^\circ)$	$^{11}D_4$	16195.999	638.446	
5A	$4f^7(^8S^\circ)5d\,(^9D^\circ)6s6p(^3P^\circ)$	$^{11}F_5$	15174.000	683.012	
5B	$4f^7(^8S^\circ)6s^26p$	$^9P_5$	15665.424	681.835	
6A	$4f^7(^8S^\circ)5d\,(^9D^\circ)6s6p(^3P^\circ)$	$^{11}F_6$	15852.245	673.259	

Before conducting the spectral scans, all possible first-step transition pathways were verified. Since some odd-parity excited states in the 28700–31000 cm^{-1} range are listed in the NIST Atomic Spectra Database, λ_2 was set to match the energy of the second-step transition, and λ_1 was scanned over a narrow range to compare the signal intensities of transitions from the ground state and various metastable states to the lower excited state. Within the acceptable wavelength range for λ_1 (610–715 nm), the first-step transition with the strongest signal intensity was selected, so that as many atoms as possible were pumped into the first excited state at a fixed laser power of $P_1 = 250$ mW. For example, for the excited state at 15665.42 cm^{-1}, the transition from the metastable level at 999.121 cm^{-1} ($\lambda = 681.835$ nm) was chosen, because the transition from 532.977 cm^{-1} was weak, and the transition from 1713.087 cm^{-1} lay outside the accessible wavelength range. During this verification, potentially interfering transitions were excluded, such as the transition from the metastable level at 215.124 cm^{-1} to the level at 16195.999 cm^{-1} ($\lambda =$ 625.748 nm), which is a representative interference pathway and is analyzed further in Subsection 3.1.

Specifically, the first excited states $4f^8 6s^2\,{}^7F_1$ at 15121.220 cm^{-1} and $4f^8 6s^2\,{}^7F_2$ at 14777.975 cm^{-1} were not employed for the scanning experiment, because no transition peaks were observed for these two levels during the verification, even when the newly identified series of energy levels was included and the delay time between the three laser beams was set to zero. According to the scanning results reported by Miyabe,[19] the $4f^8 6s^2\,{}^7F_1$ yielded only one odd-parity excited state at 33037.80 cm^{-1}, whereas the $4f^7(^8S^\circ)5d\,(^9D^\circ)6s6p(^3P^\circ)\,{}^9F_1$ at 17227.969 cm^{-1} yielded 16 excited states. This suggests that the first-step transition is extremely weak, perhaps approaching forbidden behavior. Therefore, the low-lying excited state with $J = 2$ in Table 1 contains only one state, and no low-lying states with $J = 1$ are included.

3. Results and discussion

3.1. Results of scanning with λ_1 blocked

The energy level structure of gadolinium is highly complex, with numerous possible resonant transition processes that can introduce substantial interference when scanning odd-parity excited states. Among these processes, the transitions induced solely by $\lambda_2 + \lambda_3$ were not eliminated by the previously described experimental design. These transitions occur when atoms populated in odd-parity metastable states absorb one or two λ_2 photons and then transition to excited states above 18600 cm^{-1}. Subsequently, the atoms absorb an ultraviolet λ_3 photon and undergo photoionization, without λ_1 absorption. To identify and exclude these pathways, an initial control scan was performed in the range of 572–708.5 nm with λ_1 blocked, with a scanning step rate of 5 pm/s. A total of 101 spectral peaks were observed, with intensities spanning three orders of magnitude.

Figure 3(a) shows the spectrum over 610–640.5 nm. Within this range, 21 transition peaks were observed. The experimental data, recorded as wavelength versus signal (mV), were plotted as a line trace to better illustrate the peak shapes and enhance readability. Because multiple closely spaced transition peaks appear in the range of 631–636.5 nm (indicated by the red box in Fig. 3(a)), an enlarged view of this region is provided in Fig. 3(b), where the separated peaks are resolved. The two strongest peaks (labels 47/48) are separated by only 8 pm.

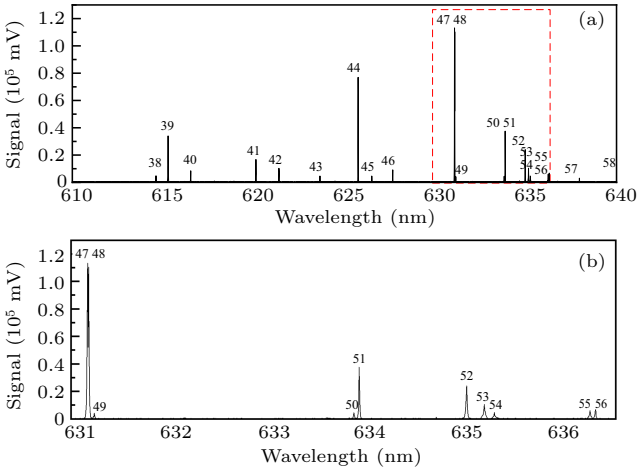


Fig. 3. Interference peaks revealed with λ_1 blocked. Panel (a) presents the 21 spectral peaks obtained from scanning the range of 610–640.5 nm, while panel 3(b) is an enlarged view of the red-boxed region in (a), containing 10 closely spaced peaks. All peaks are labeled according to the numbering in the supplementary data.

For all the spectral peaks obtained with λ_1 blocked, the signal intensities were normalized to the scanning λ_2 power, with detailed data recorded in the supplementary data. Based on the NIST Atomic Spectra Database and prior reports on Gd excited levels,[18–21,27] the transition pathways corresponding to these peaks were analyzed. Specifically, the photon energies of the observed peaks were matched to processes where atoms in odd-parity ground and metastable states absorb one λ_2 photon to reach even-parity excited states before ionization, or absorb two λ_2 photons to reach higher odd-parity excited states before ionization.

Table 2 summarizes the transition assignments for the 12 peaks with normalized intensities exceeding 50000. The three strongest transitions all originate from the first metastable state. Peaks 47 and 48 in Fig. 3 correspond, respectively, to (i) a first-step resonance from the first metastable state to 16061.273 cm^{-1} followed by a near-resonant second step to the odd-parity level at 31907.02 cm^{-1}, and (ii) a two-photon λ_2 resonance directly populating the same 31907.02 cm^{-1} level. Peak 44 in Fig. 3 likewise follows the first-step-resonant/second-step-near-resonant pathway, analogous to peak 47, whereas no peak attributable to a two-photon λ_2 resonance was observed.

Table 2. Twelve strongest peaks (normalized intensity >50000) observed with λ_1 blocked and their assigned transition pathways.

Number	λ_2 (nm)	Signal (arb. units)	Initial		First step			Second step		
			E_1 (cm^{-1})	J_1	E_2 (cm^{-1})	J_2	Δ_1 (cm^{-1})	E_3 (cm^{-1})	J_3	Δ_2 (cm^{-1})
1	631.067	18.033	215.124	3	16061.273	3	–0.03	31907.020	3	–0.43
2	631.079	17.133	215.124	3		/		31907.020	3	0.06
3	625.748	14.017	215.124	3	16195.999	4	0.00	32176.447	4	–0.42
4	677.645	9.611	6786.184	4	21543.156	3	–0.02		/	
5	573.877	8.150	7234.910	4	24660.325	5	0.09		/	
6	646.149	7.100	6976.508	5	22452.867	6	0.05		/	
7	708.395	7.088	7426.710	3	21543.156	3	0.02		/	
8	681.644	6.611	7234.910	4	21905.353	5	0.04		/	
9	651.490	5.986	7103.420	5	22452.867	6	0.02		/	
10	615.278	5.680	6976.508	5	23229.298	6	–0.02		/	
11	633.861	5.679							/	
12	582.072	5.100	7480.348	6	24660.325	5	–0.01		/	

Most other peaks arise from atoms in higher metastable states, which are first excited to even-parity levels above 20000 cm^{-1} and then absorb an ultraviolet λ_3 photon to exceed the ionization threshold. For all 101 spectral peaks discovered during the scan, the above analysis was carried out, and transition assignments were made for 87 peaks, as documented in the supplementary data. Of these, 4 peaks (numbered 6, 19, 50, and 59) were found to have two possible transition processes. The largest deviation between the measured photon energies and literature values was -0.11 cm^{-1}, with most deviations within ± 0.05 cm^{-1}. These results indicate high scan accuracy, and no significant systematic offsets were evident.

In analyzing the transition processes corresponding to the spectral peaks, it was found that most peaks arose from atoms in higher metastable states undergoing a "first-step resonance + ultraviolet photoionization" pathway. Only 10 peaks were likely to arise from transitions involving the direct absorption of two resonant photons. This outcome contrasts with the single-color multiphoton ionization spectra of gadolinium reported by Miyabe,[25] where most of the 72 transition lines originated from direct two-photon absorption from the ground or low-lying metastable states to odd-parity highly excited states, similar to peak 2 in Table 2.

The differences are due to the following factors:

1. In our experiment, ionization was driven by an ultraviolet laser at 322.5 nm, capable of directly ionizing atoms in even-parity excited states above 20000 cm^{-1}. By contrast, Miyabe's study used light in the 530–635 nm range, insufficient to ionize atoms from these states.

2. The photoionization cross section decreases rapidly as energy rises above the ionization threshold.[28–30] In our experiment, transitions from odd-parity excited states in the 32000–35000 cm^{-1} range terminated in final states more than 1.66 eV above threshold, whereas Miyabe's transitions ended only 0–0.2 eV above threshold, favoring photoionization from odd-parity states in their case.

3. Gadolinium atoms possess dense autoionizing Rydberg states near the ionization threshold,[20] making near-threshold photoionization more probable. In our experiment, slight adjustments to the ionization wavelength significantly affected the intensity of some peaks. Figure 4 compares scans in the 651–656.5 nm range for $\lambda_3 = 322.5$ nm and 322.55 nm. Although the transition wavelengths were identical, peaks 67–69 displayed marked intensity differences, suggesting that ionization was enhanced by near-resonant processes. This effect was especially evident for the strong peaks in Table 2. Nevertheless, because research on gadolinium's autoionizing states remains scarce, further data are needed to analyze these near-resonant processes in detail.

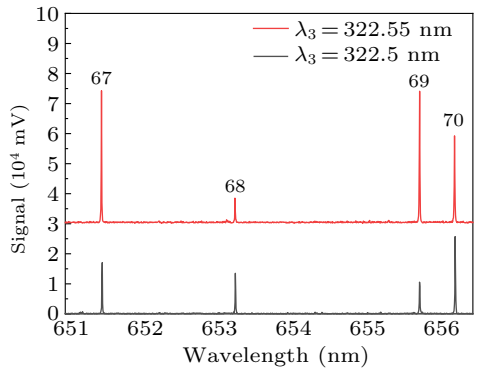


Fig. 4. Effect of λ_3 on peak intensities. Scans over 651–656.5 nm are compared for $\lambda_3 = 322.50$ nm and 322.55 nm. Although transition wavelengths are consistent, peaks 68 and 69 show pronounced intensity changes, indicating near-resonant enhancement of the ionization step.

Additionally, as shown by transition 11 ($\lambda = 633.861$ nm) in Table 2, whose transition pathway has remained unassigned, 14 peaks in the supplementary data still lack identified transition processes. This is likely due to the absence of certain even-parity excited states or high-lying odd-parity excited states in the current scan. By calculating the energy differences between the remaining peaks and matching them with the low-lying metastable states of gadolinium, possible transition pathways are hypothesized. For example, the stronger transition peaks at $\lambda = 633.861$ nm and 623.650 nm are likely due to transitions from the metastable states at 7234.910 cm^{-1} and 6976.508 cm^{-1} to the even-parity excited state at 23011.19 cm^{-1}, which is expected to have $J = 4$ or 5. Similarly, the peaks at $\lambda = 595.492$ nm and 573.611 nm

may have shared a common final state at 24215.59 cm^{-1}, with $J = 3$ or 4. To conclusively verify the existence of these levels, it is necessary to use multicolor pump–probe techniques to identify the corresponding initial states,[25] which is beyond the scope of the present study.

3.2. Results of odd-parity excited states

After the potential interference transitions were identified, the odd-parity excited state regions for all nine lower levels were scanned according to the first-step transitions listed in Table 1. Figure 5(a) shows the spectrum over 651–675 nm for excitation from 16061.273 cm^{-1} (labeled as 3C in Table 1). Five relatively strong peaks, together with a series of weaker features, are observed. Figure 5(b) provides the detail for signals below 50000 mV, and Fig. 5(c) zooms in on the two closely spaced peaks at 653.3 nm, which are highlighted by the yellow box in Fig. 5(b).

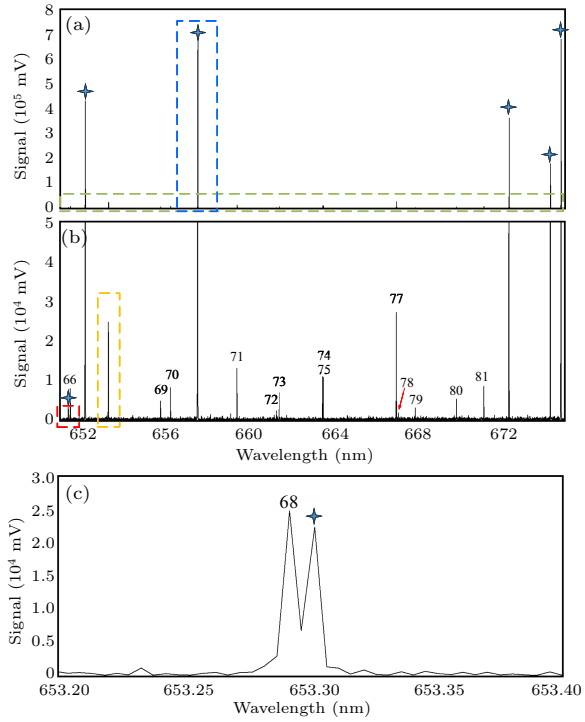


Fig. 5. Spectrum for excitation from the even-parity excited state at 16061.273 cm^{-1} over 651–675 nm. (b) Enlargement of the green-boxed region in panel (a), showing signals < 50000 mV that are dominated by interference lines. (c) Zoom of the closely spaced doublet at 653.3 nm (yellow box in (b)). Seven peaks formed by transitions to odd-parity excited states are marked with blue asterisks; the other 14 interference peaks are numbered as in the supplementary data. The strongest and weakest resonances (blue and red boxes) are fitted with Voigt profiles in Fig. 6. Exclusion of interference peaks identified in λ_1-blocked scans is essential for confirming odd-parity levels.

After the 14 interfering transitions confirmed in Subsection 3.1 were excluded (as labeled in the supplementary data), the remaining seven peaks may correspond to transitions between the selected even-parity and higher odd-parity excited states, marked with blue asterisks. These results show that interference peaks substantially outnumber those attributable to transitions to odd-parity excited states. Moreover, the intensities of the odd-parity peaks span a wide range; the two weakest are comparable to the interference peaks, underscoring the need to exclude interference.

Control tests were performed on transition peaks that might correspond to odd-parity excited states under three conditions: λ_1 blocked, λ_3 blocked, and λ_3 detuned by 50 pm. The expected outcome was that signals vanished when either λ_1 or λ_3 was blocked, whereas a 50 pm detuning of λ_3 did not shift the peak positions. These results are consistent with a mechanism of two-step resonant excitation followed by non-resonant ultraviolet (UV) photoionization in the third step.

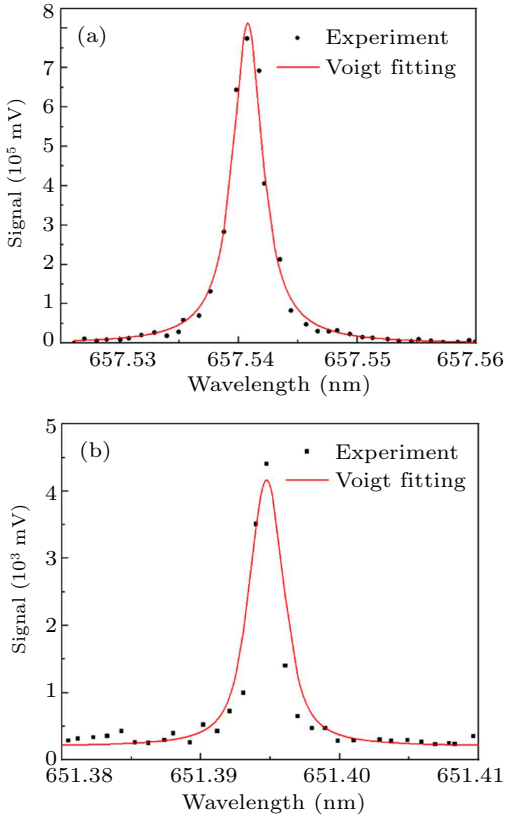


Fig. 6. Voigt-profile fits for the strongest and weakest resonances highlighted in Figs. 5(a) and 5(b), marked with blue and red boxes, respectively. Through multiple scans and fitting procedures, precise energy level positions and uncertainties were obtained, with detailed data provided in the supplementary data.

Following these checks, multiple scans with a step rate of 1 pm/s were performed within ±50 pm of the peak center. Peak centers were determined by Voigt-profile fitting, and the corresponding energy positions were derived. Figures 6(a) and 6(b) show the Voigt fitting results for the strongest and weakest transition peaks in Fig. 5, marked with blue and red boxes, respectively. Thus, by scanning from selected even-parity lower states, a series of odd-parity excited states with precisely determined energy positions were obtained.

The energy positions, uncertainties, transition center wavelengths, and λ_2-power-normalized signal intensities for all nine even-parity lower states are provided in the supplementary data. Note that the normalized intensities across dif-

ferent even-parity states were not compared, because most transitions remained unsaturated at $P_1 = 250$ mW. Due to the relatively low laser power and differences in transition intensities, the number of atoms pumped into the even-parity excited states varied, preventing a meaningful comparison of the normalized signal intensities for different E_1 values. Additionally, the λ_3 wavelength setting significantly affected the signal intensities of some transitions, suggesting the possible presence of near-resonant enhanced ionization processes.

The angular momentum of the odd-parity excited states was confirmed by scanning the same energy region from different even-parity lower levels. In addition, by averaging the energy positions derived from scans originating from multiple even-parity levels within a given region, precise energy positions were obtained. These positions were then compared with the NIST Atomic Spectra Database and prior literature to determine whether the levels were newly identified.

Figure 7 shows the results for the 30500–31500 cm^{-1} region, obtained by scanning from five even-parity levels with $J = 2$–6. Interfering transitions were excluded based on the results of Subsection 3.1, and all peaks in the figure therefore correspond to genuine odd-parity excited states. For multiple even-parity levels with the same J value (e.g., levels 3A, 3B and 3C in Table 1), only one representative trace is shown. The signal intensities were normalized to the λ_2 power, consistent with the supplementary data. For five very weak lines, their signal intensities are scaled by $\times 10$ and highlighted in blue boxes. Within this region, scans from multiple lower levels identified 18 odd-parity excited states. With the exception of a few levels seen only in the $J = 2$ and $J = 6$ scans, all were observed from multiple lower levels, providing strong verification for the authenticity of these energy levels.

For J assignment, taking the odd-parity excited states at 30934.652 cm^{-1} and 30951.153 cm^{-1}, indicated by the red dashed lines in Fig. 7, as examples, transitions from three distinct even-parity lower levels were found to converge on the same odd-parity upper level. By applying the electric-dipole selection rules to the known lower-level J values, the J values of these two odd-parity excited states were uniquely assigned as $J = 3$ and $J = 5$, respectively. Using this approach, J was assigned for all scanned odd-parity levels.

Notably, the odd-parity excited state at 31412.955 cm^{-1} ($J = 2$) was observed from all three $J = 3$ lower levels but not from the $J = 2$ lower level at 14036.026 cm^{-1}, likely because the transition strength from the latter was extremely weak. A similar situation was observed for the odd-parity excited state at 30042.675 cm^{-1}. In addition, substantial intensity differences were observed for the same odd-parity level when scanned from different even-parity lower levels — even for identical J — underscoring the need to scan each region via multiple lower levels.

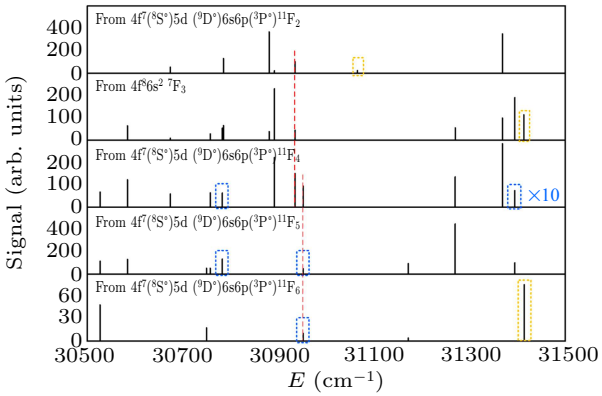


Fig. 7. Odd-parity excited states from scans of 30500–31500 cm^{-1} using five even-parity lower levels with $J = 2$–6. The initial levels are indicated in each subfigure. Very weak lines are scaled $\times 10$ and highlighted with blue boxes. Red dashed lines mark the levels at 30934.652 cm^{-1} and 30951.153 cm^{-1}, each accessible from three distinct lower J, enabling unique assignments $J = 3$ and $J = 5$. Apart from two levels seen only in $J = 2$ or $J = 6$ scans and the level at 31412.955 cm^{-1} (both highlighted by yellow box), all odd-parity excited states in this figure are confirmed from multiple lower levels.

A total of 40 odd-parity excited states were observed in the 28700–31500 cm^{-1} range. The energy positions (E), standard error (SE), angular momenta (J), corresponding lower levels, and comparison with literature data are listed in Table 3. The energy positions and standard errors were obtained through two rounds of weighted averaging: First, spectra originating from a specific lower energy level in Table 1 were fitted using a Voigt profile for the peaks corresponding to the odd-parity excited states, as shown in Fig. 7, providing multiple sets of energy positions and standard errors. A weighted average was then calculated using the standard errors as weights to determine the average energy position and standard error for the excited states from the corresponding lower energy level, recorded in the supplementary data. For excited states appearing in spectra from multiple lower energy levels, the average uncertainty from each energy level was used as a weight to calculate a second weighted average, resulting in the precise energy positions and standard errors listed in Table 3.

Below 31000 cm^{-1}, 14 of these levels are recorded in the NIST Atomic Spectra Database,[27] whereas above 31000 cm^{-1} all seven observed levels agree with the values reported by M. Miyabe.[19] The remaining 19 odd-parity excited states are newly reported, predominantly concentrated in the 30500–31000 cm^{-1} range. The largest uncertainty among the present level energies is 0.013 cm^{-1}, with most below 0.005 cm^{-1}. The uncertainty mainly arises from the influence of variations in laser power and atomic flow density on the fitted peak shapes. Additionally, after weighted averaging, the standard errors for some excited states, derived from scans of only one lower energy level, are significantly higher than those for states obtained from multiple lower energy levels. Agreement with NIST is excellent: the maximum deviation is -0.063 cm^{-1} at 29041.709 cm^{-1}, and 11 levels have $|\Delta| < 0.02$ cm^{-1}, demonstrating the accuracy of the present

data. Differences relative to Miyabe are slightly larger: for six levels the mean deviation is 0.04 cm^{-1}, within their stated precision of ± 0.1 cm^{-1}; however, at 31064.810 cm^{-1} the deviation reaches 0.26 cm^{-1}, which may reflect systematic effects in their experiment together with possible isotope-shift contributions. Since this level has $J = 1$, cross-verification by scans from alternative lower levels was difficult.

Regarding J assignment, and based on the electric-dipole selection rule, the angular momenta of all 40 odd-parity excited states were assigned. For the 14 levels whose energy positions agree with the NIST Atomic Spectra Database, the J assignments were also identical. For the levels reported by Miyabe, the levels at 31064.810 cm^{-1} and 31413.671 cm^{-1} were uniquely assigned $J = 1$ and $J = 7$, respectively.

In addition, because no transitions to the 31236.74 cm^{-1} excited state reported by Miyabe were observed in scans from $J = 2$ or $J = 3$ lower levels, its J was tentatively assigned as 0. The J assignments for the remaining levels were mutually consistent. Among the 19 newly observed levels, 18 received unique J assignments. However, the level at 30042.675 cm^{-1} was not observed in the $J = 2$ or $J = 4$ lower-level scans, so a unique J could not be determined. The possible J values for this level were 2, 3, or 4. Similarly, for the levels at 31412.955 cm^{-1} ($J = 2$) and 30367.361 cm^{-1} ($J = 7$), no transitions were observed from the lower levels $4f^7(^8S^\circ)5d\ (^9D^\circ)6s6p(^3P^\circ)\ ^{11}F_2$ and $^{11}F_6$, which was likely owing to very weak transition strengths.

Table 3. Odd-parity excited states observed between 28700 cm^{-1} and 31500 cm^{-1}: energy positions (E), standard error (SE), J, lower levels used for assignment, and comparison with literature. The energy positions and their uncertainties are weighted averages across scans from different even-parity starting levels.

No.	E_{avg} (cm^{-1})	SE (cm^{-1})	J	Corresponding lower levels	NIST database[27]		M. Miyabe[19]		Δ (cm^{-1})
					E (cm^{-1})	J	E (cm^{-1})	J	
1	28725.108	0.003	2	2A, 3A, 3B	28725.150	2	/		–0.042
2	28741.538	0.011	1	2A	28741.590	1	/		–0.052
3	28745.100	0.007	4	3A, 3B			/		
4	28837.241	0.006	5	4A	28837.240	5	/		0.001
5	28938.298	0.006	5	4A	28938.287	5	/		0.011
6	29041.709	0.002	3	2A, 3A, 3B, 4A	29041.772	3	/		–0.063
7	29143.536	0.006	2	2A, 3A, 3B			/		
8	29174.564	0.004	4	3A, 3B, 4A	29174.580	4	/		–0.016
9	29312.752	0.004	5	4A, 5A	29312.770	5	/		–0.018
10	29420.660	0.006	6	5A	29420.675	6	/		–0.015
11	29439.322	0.004	5	4A, 5A	29439.330	5	/		–0.008
12	29464.174	0.009	1	2A			/		
13	29568.782	0.002	3	2A, 3A, 4A			/		
14	29672.499	0.005	4	3A, 3B, 4A, 5A	29672.515	4	/		–0.016
15	29779.927	0.003	5	4A, 5A, 5B			/		
16	29867.532	0.003	6	5A, 5B	29867.535	6	/		–0.003
17	29891.739	0.002	4	3A, 3B, 4A, 5A			/		
18	30042.675	0.006	2/3/4	3A,3B			/		
19	30197.070	0.003	3	2A, 3A, 3B, 4A			/		
20	30248.607	0.013	1	2A					
21	30289.374	0.001	4	3A, 3B, 3C, 4A, 5A, 5B	30289.386	4	/		–0.012
22	30457.409	0.002	2	2A, 3A, 3B, 3C			/		
23	30526.537	0.002	5	4A, 4B, 5A, 5B, 6A					
24	30583.735	0.001	4	3A, 3B, 3C, 4A, 4B, 5A, 5B	30583.740	4	/		–0.005
25	30673.345	0.002	3	2A, 3A, 3B, 3C, 4A, 4B			/		
26	30749.175	0.002	6	5A, 5B, 6A	30749.194	6	/		–0.019
27	30757.010	0.001	4	3A, 3B, 3C, 4A, 4B, 5A, 5B			/		
28	30782.140	0.002	4	3A, 3B, 3C, 4A, 5A, 5B			/		
29	30784.503	0.003	2	2A, 3A, 3B, 3C,			/		
30	30880.150	0.001	2	2A, 3A, 3B, 3C			/		
31	30891.372	0.001	3	2A, 3A, 3B, 3C, 4A, 4B			/		
32	30934.652	0.003	3	2A, 3A, 3B, 3C, 4A, 4B			/		
33	30951.153	0.002	5	4A, 4B, 5A, 5B, 6A					
34	31064.810	0.003	1	2A	/		31064.550	1,2	0.260
35	31171.124	0.002	6	5A, 5B, 6A	/		31171.070	6	0.054
36	31269.452	0.002	4	3A, 3B, 3C, 4A, 4B, 5A, 5B	/		31269.370	4	0.082
37	31368.125	0.002	3	2A,3A,3B,3C,4A,4B	/		31368.080	3	0.045
38	31394.096	0.002	4	3A, 3B, 3C, 4A, 4B, 5A, 5B	/		31394.010	4	0.086
39	31412.955	0.002	2	3A, 3B, 3C	/		31412.980	2	–0.025
40	31413.671	0.005	7	6A	/		31413.670	6,7	0.001

4. Conclusions

A three-color, three-step photoionization scheme was employed to investigate the odd-parity excited states of gadolinium in the 28700–31500 cm^{-1} range. Potential interference peaks were identified through a scan with λ_1 blocked over 572–708.5 nm. A total of 101 spectral lines were observed, and transition pathways were assigned for most of them. By scanning the energy region for 9 even-parity levels with different J values, 40 odd-parity excited states were identified, including 19 newly reported. The J values of these levels were determined based on the electric-dipole selection rule. Comparison with the NIST Atomic Spectra Database and prior studies confirms the high accuracy of present level energies. These results provide a new data set for odd-parity excited states of gadolinium, expand the understanding of gadolinium's atomic level structure, and contribute to theoretical calculations of lanthanide atoms and multi-element astrophysical modeling.

Data availability statement

The data presented in this paper are openly available in Science Data Bank at https://doi.org/10.57760/sciencedb.33295.

The supplementary data for this study, which include detailed results from the scanning of odd-parity excited states using nine even-parity levels, along with data for interference peak exclusion and transition process analysis, are available. Additional data sets generated during the current study are available from the corresponding author on reasonable request.

Acknowledgement

This research was supported by the Tianjin Science and Technology Program Project (No. 24ZXZSSS00530).

References

[1] Peper M, Li Y, Knapp D Y, Bileska M, Ma S, Liu G, Peng P, Zhang B, Horvath S P, Burgers A P and Thompson J D 2025 *Phys. Rev. X* **15** 011009

[2] Hovhannesyan G and Lepers M 2023 *Phys. Scr.* **98** 025407

[3] Klempka M, Elantkowska M, Furmann B, Ruczkowski J, Głowacki P, Mieloch S and Stefańska D 2025 *J. Quant. Spectrosc. Radiat. Transf.* **347** 109632

[4] Sahoo A C, Mandal P K, Mukherjee J, Dev V and Shah M L 2022 *J. Quant. Spectrosc. Radiat. Transf.* **292** 108352

[5] D'yachkov A B, Gorkunov A A, Labozin A V, Mironov S M, Firsov V A, Tsvetkov G O and Panchenko V Ya 2023 *Bull. Lebedev Phys. Inst.* **50** S187

[6] Fujiwara T, Kobayashi T and Midorikawa K 2019 *Sci. Rep.* **9** 1754

[7] Luck R E, Kovtyukh V V and Andrievsky S M 2006 *Astron. J.* **132** 902

[8] Nahar S N and Hinojosa-Aguirre G 2024 *Atoms* **12** 22

[9] Guiglion G, De Laverny P, Recio-Blanco A and Prantzos N 2018 *Astron. Astrophys.* **619** A143

[10] Nahar S N 2024 *Atoms* **12** 24

[11] Mishenina T, Pignatari M, Gorbaneva T, Cote B, Lopez A Y, Thielemann F K and Soubiran C 2022 *Mon. Not. Roy. Astron. Soc.* **516** 3786

[12] Den Hartog E A, Lawler J E, Sneden C and Cowan J J 2006 *Astrophys. J. Suppl. Ser.* **167** 292

[13] Spina L, Meléndez J, Karakas A I, Santos L D, Bedell M, Asplund M, Ramírez I, Yong D, Alves-Brito A, Bean J L and Dreizler S 2017 *Mon. Not. Roy. Astron. Soc.* **474** 2580

[14] Niki H, Motoki K, Yasui M, Horiuchi Y, Tokita S and Izawa Y 2006 *J. Nucl. Sci. Technol.* **43** 427

[15] Sankari M and Suryanarayana M V 2015 *J. Nucl. Eng. Radiat. Sci.* **1** 041017

[16] Sankari M, Suryanarayana M V and Gangadharan S 1999 *J. Nucl. Mater.* **264** 122

[17] Van Kleef Th A M, Blaise J and Wyart J F 1971 *J. Phys. France* **32** 609

[18] Qu J N, Zhou Z Y, Zhu L Z, Lin F C 1991 *Chin. J. Lasers* **18** 659

[19] Miyabe M, Wakaida I and Arisawa T 1996 *J. Phys. B: At. Mol. Opt. Phys.* **29** 4073

[20] Miyabe M, Oba M and Wakaida I 1998 *J. Phys. B: At. Mol. Opt. Phys.* **31** 4559

[21] Jim-Tae K, Jonghong Y, Yongjoo R, Jongmin L 2000 *J. Korean Phys. Soc.* **37** 701

[22] Zhang J Y, Xiong J Y, Wei S Q, Li Y F and Lu X Y 2023 *Acta Phys. Sin.* **72** 193203 (in Chinese)

[23] Zhang J Y, Lu X Y, Li Y F and Chai J J 2024 *Eur. Phys. J. D* **78** 95

[24] Zhang J Y, Xiong J Y, Zhou H R, Zhu C H, Sun H M, Wang L D, Chai J J and Li Y F 2025 *Spectroc. Acta Pt. B-Atom. Spectr.* **231** 107249

[25] Miyabe M and Wakaida I 1997 *J. Phys. B: At. Mol. Opt. Phys.* **30** 4193

[26] Miyabe M, Wakaida I and Arisawa T 1997 *Z. Phys. D-Atoms Mol. Clusters* **39** 181

[27] Kramida A, Ralchenko Yu, Reader J, NIST ASD Team 2024 NIST Atomic Spectra Database (ver. 5.12) [Online]. 2025, Gaithersburg, MD: National Institute of Standards and Technology. DOI: 10.18434/T4W30F

[28] Zhang Z M, Wang Z C, Wang Q L, Ma X K, Wang Z X, Hua Z X, Yao G X, Yang X Y, Sun Z F, Qin Z B and Zheng X F 2024 *J. Chem. Phys.* **160** 164201

[29] Elizarov A Y and Tupitsyn I I 2007 *J. Phys. B: At. Mol. Opt. Phys.* **40** 1991

[30] Yar A, Ali R and Baig M A 2013 *Phys. Rev. A* **88** 033405